Fundamental Experiments on a Reinforcement Method using Sheet Pile Wall for Bridge Pile Foundations Subjected to Pile Embedment Reduction and Numerical Validation

T. Tikanta[1], T. Matsumoto[2], A. T. Vu[3], S. Kobayashi[4], S. Shimono[5] and C. Bamrungwong[6]
[1]*Department of Rural Roads, Ministry of Transportation, Chiang Mai, Thailand*
[2,4,5]*Graduate School of Natural Science and Technology, Kanazawa University, Kanazawa, Japan*
[3]*Le Quy Don Technical University, Hanoi, Vietnam (former PhD student at Kanazawa University)*
[6]*Department of Rural Roads, Ministry of Transportation, Bangkok, Thailand*
[1]*E-mail:* tanatantikanta@gmail.com
[2]*E-mail:* matsumoto@se.kanazawa-u.ac.jp
[3]*E-mail:* vuanhtuan@mta.edu.vn
[4]*E-mail:* koba@se.kanazawa-u.ac.jp
[5]*E-mail:* shimono@se.kanazawa-u.ac.jp
[6]*E-mail:* chakreeb@gmail.com

ABSTRACT: Development of an effective countermeasure for existing bridge foundations subjected to the influence of riverbed excavation in Thailand is the main objective of this research. Due to the riverbed soil excavation for the utilization in construction works for many years, the level of riverbed of the Mae Nam Ping River has been considerably decreased, resulting in reduction of embedment lengths of piles for many bridge foundations. Erosion was not a cause of the lowering of the riverbed. Reductions of bearing capacity due to the lowering of riverbed soil is the main cause of bridge pile foundation settlements or collapses at present. In order to prevent the damages of existing bridge pile foundations caused by the riverbed soil excavation, a reinforcement method using sheet piles called "Sheet Pile Wall (SPW) reinforcement" is proposed in this paper. The proposed SPW reinforcement method consists of 2 simple steps without new additional piles or any modifications of existing structures. Firstly, sheet piles are constructed surrounding the existing problematic bridge pile foundation. Finally, the empty space inside the SPW is filled with sand or other porous materials such as crushed concrete. In order to investigate the performance of the proposed SPW reinforcement method, series of load tests on model pile foundations in dry sand were carried out. The experimental results show that the proposed SPW reinforcement method is very efficient and promising. Numerical simulation of an experiment using FEM was also carried out to get more insight into the mechanism of the SPW method and validate the proposed SPW method.

KEYWORDS: Reinforcement, Existing bridge pile foundation, Riverbed soil excavation, Model load test, Numerical analysis

1. INTRODUCTION

In the past decade, the Mae Nam Ping River crossing bridges in Chiang Mai and Lamphun, located in the northern area of Thailand (Figure 1), encountered pile foundation damages frequently.

Figure 1 Location of the Mae Nam Ping River in Chiang Mai and Lamphun, Thailand

Figure 2 shows the first case of bridge foundation damage in 2006. One of pile foundations of the bridge LP.010 in Lamphun settled during a high flood season. The investigation and arrangement for the solution were performed for 2 years. The settled bridge LP.010 was repaired in 2008 by using new additional piles, extension of the footing, jacking up the bridge girders and extending the height of the settled bridge pier by 0.80 m to keep flat level of the bridge slabs as shown in Figure 3.

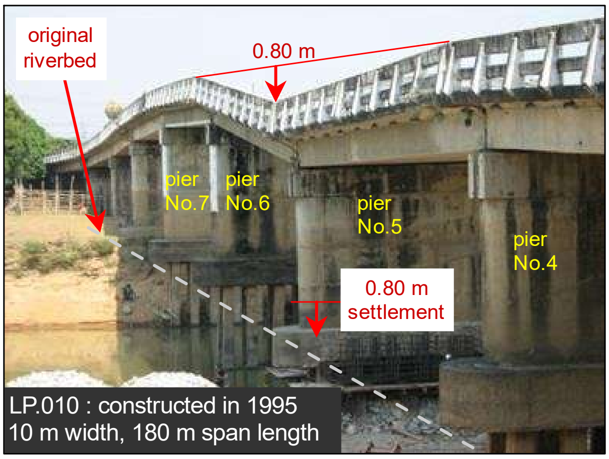

Figure 2 Differential settlement of the bridge LP.010 in Lamphun, Thailand (2006)

Figure 3 Repair of the settled bridge LP.010 in Lamphun, Thailand (2008)

A few years later, another pile foundation at the pier No.7 of the same bridge LP.010 settled again during a high flood season in 2010. This time, the settled pile foundation collapsed and fell down into the river within 5 days after the settlement. The collapsed bridge LP.010 was repaired in 2013 by constructions of 2 new pile foundations at new locations on both sides of the previously collapsed pier No.7 (see Figure 3). In the same year of 2010, two other bridges crossing the Mae Nam Ping River named CM.015 and CM.025 also encountered the differential settlement problem. Both of them were repaired in 2013 by the similar way as the repair of the previous settled bridge (LP.010).

The main cause of the bridge foundation damages mentioned above was the lowering of riverbed soil, in other words, the reduction of pile embedment length. Though the damaged bridges were repaired, most of undamaged bridge pile foundations along the river still have potential risks of damaging due to the riverbed soil excavation as shown in Figure 4. It should be noted here that excavation of the riverbed is prohibited by regulation at present, hence further reduction of pile embedment length will not occur.

Figure 4 An example case of undamaged bridge which has potential risk of damaging (2012)

Although the repairs of the damaged bridge were successful, the repair method cannot be applied to the reinforcement of many undamaged bridge foundations, because of a high cost and a long construction time of the repair method in which additional piles and extension of footing are required. Hence, in order to obtain an efficient countermeasure for the existing bridge pile foundations subjected to the problem of riverbed soil excavation, a fundamental experimental study was carried out in this research. Considering safety, economic and uncomplicated approach, a reinforcing method using sheet pile wall (SPW) called "SPW reinforcement" (SPW method, hereafter) is proposed.

Figure 5 illustrates the concept of SPW reinforcement method. The construction procedure of SPW reinforcement consists of 2 simple steps without new additional piles or any modifications of existing structures. Firstly, a permeable sheet pile wall is constructed surrounding the existing problematic bridge pile foundation. Finally, the empty space inside the SPW is filled with sand or other porous materials such as crushed concrete.

A method for reinforcing an existing pile foundation by means of sheet pile wall, called In-cap Method, has been proposed by Fukuda et al. (2005). The In-cap method surrounds the existing foundation footing to a required depth, solidifies the soil inside of the sheet piles for improvement of the bearing capacity of the footing and integrates the improved footing with the existing foundation.

The SPW reinforcement method proposed in this paper has similar feature to the In-cap Method, however, a big difference between the two methods is that no soil (ground) exists around the sheet pile wall in the SPW reinforcement method. The shape of the proposed SWP reinforcement method is similar to that of a coffer dam. A feature of the SPW method is to use permeable sheet pile wall in order to minimise the interference of river stream.

Hence, investigation of the reinforcement mechanisms in the SPW method is carried out in this research.

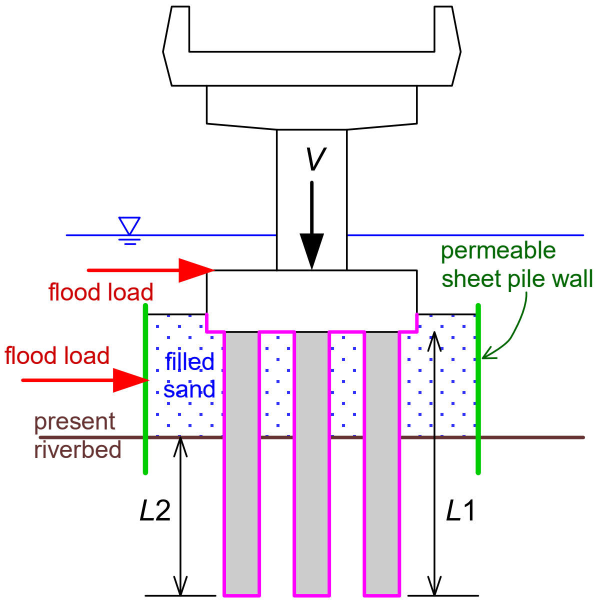

Figure 5 A concept of Sheet Pile Wall (SPW) reinforcement method

In this study, series of vertical load tests on small-sized model pile foundations at 1-g field were carried out to demonstrate the validity of the SPW method and to investigate the mechanism of the SPW method, because the actual damages of the bridge foundations in Thailand were caused by large settlements with little horizontal displacement. Numerical simulation of an experiment using FEM was also carried out to get more insight into the mechanism of the SPW method and validate the proposed SPW method.

2. EXPERIMENT DESCRIPTION

The ground conditions and the foundation configurations of the actual bridges are various. Hence, the aim of the experiments is not to simulate the conditions of the actual bridge pile foundations precisely, but to demonstrate the validity of the SPW method and to investigate the mechanism of the SPW method thorough small-sized model tests.

Series of model load tests on a single pile, 3-pile pile foundation and 4-pile pile foundation were carried out.

2.1 Model piles and model pile foundations

An aluminum pipe having 32 mm diameter with 600 mm length as shown in Figure 6 was employed as model pile in the single pile load tests. Strain gauges were instrumented along the pile shaft to obtain axial forces during the load tests. Sand particles were glued on the pile shaft to increase shaft friction and to protect strain gauges from damage. An end cap was not attached to the pile tip so that the pile had open-ended condition. Physical and mechanical properties of the model single pile are listed in Table 1. Young's modulus, E_p, and Poisson's ratio, ν_p, were estimated from the compression tests of the model pile.

Aluminum pipes having 20 mm diameter with 285 mm length as shown in Figure 7 were employed as model piles in the 3-pile and 4-pile pile foundations. Each model pile was instrumented with strain gauges and was glued with sand particles as similar to the model single pile. An end cap was attached to the pile tip so that the pile had close-ended condition. Physical and mechanical properties of the model piles are listed in Table 2.

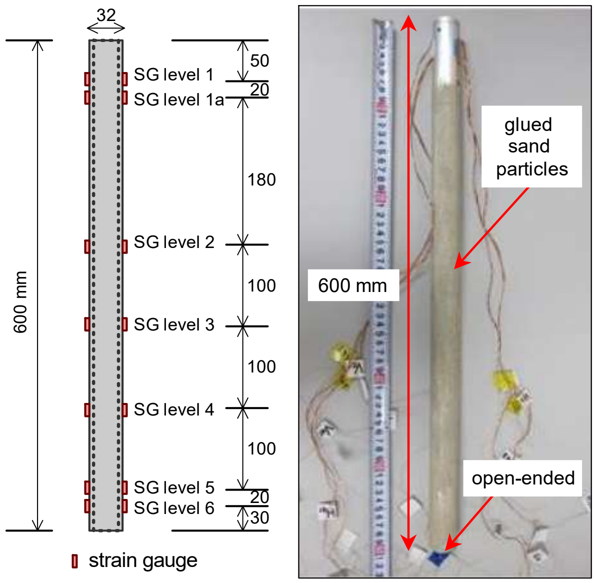

Figure 6 Configurations of the model pile for single pile load tests

Table 1 Physical and mechanical properties of the model single pile

Item	Value
Pile length, L_p (mm)	600
Outer diameter, D_o (mm)	32
Inner diameter, D_i (mm)	29.3
Wall thickness, t_w (mm)	1.35
Density, ρ_p (g/cm^3)	2.70
Young's modulus, E_p (MPa)	65,400
Poisson's ratio, ν_p	0.33

Figures 8 and 9 show the configurations and dimensions of the 3-pile pile foundation and the 4-pile pile foundation, respectively. The pile caps or rafts of both model foundations are made of aluminum alloy, which have specifications listed in Tables 3 and 4.

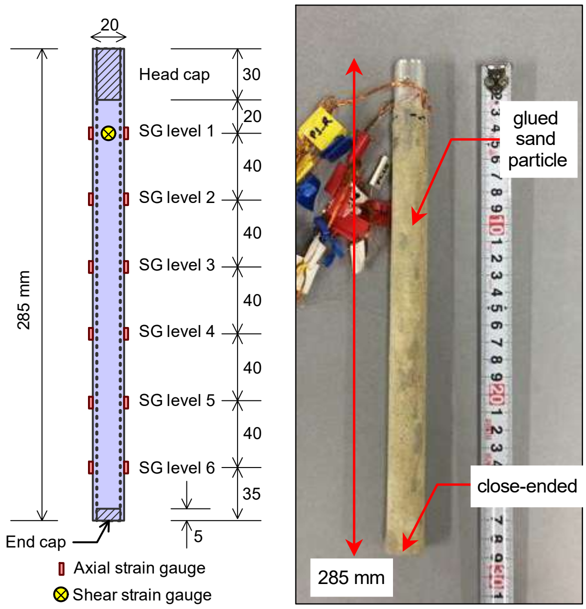

Figure 7 Configurations of the model piles consisted in 3-pile and 4-pile pile foundations

Table 2 Physical and mechanical properties of the model piles consisted in the model pile foundations

Item	Value
Pile length, L (mm)	285
Outer diameter, D_o (mm)	20
Inner diameter, D_i (mm)	17.8
Wall thickness, t (mm)	1.1
Density, ρ (g/cm^3)	2.70
Young's modulus, E (MPa)	65,000
Poisson's ratio, ν	0.33

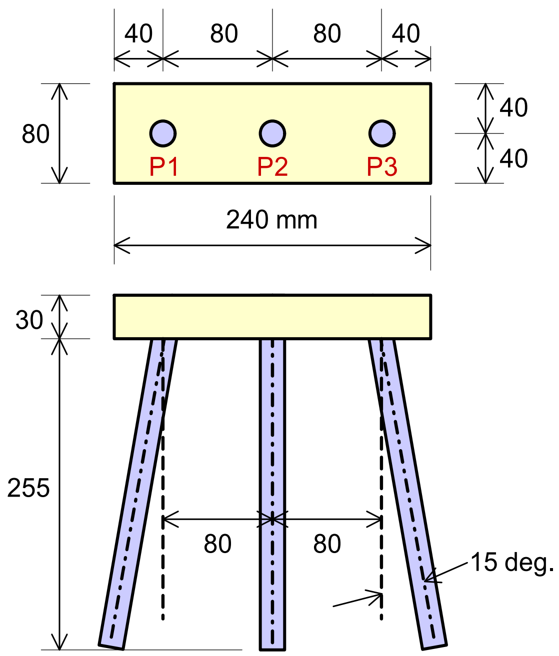

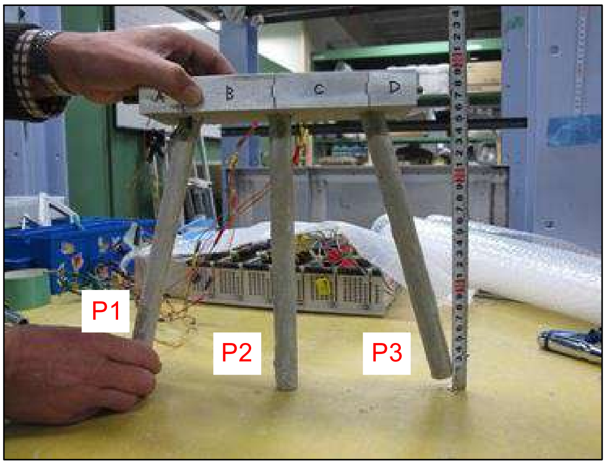

Figure 8 Configurations of the 3-pile pile foundation model

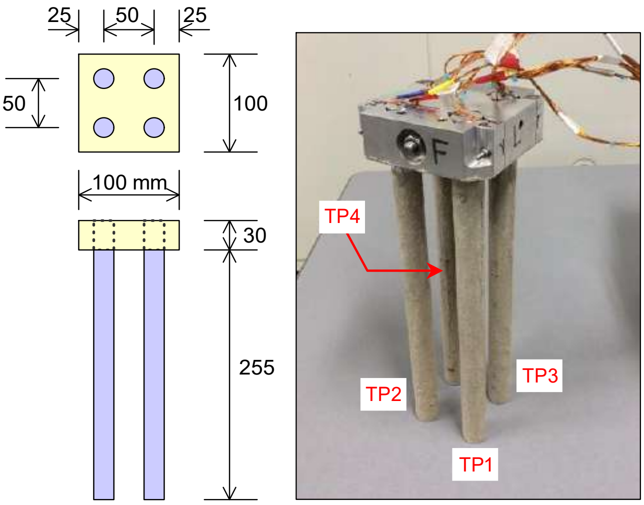

Figure 9 Configurations of the 4-pile pile foundation

Table 3 Physical and mechanical properties of the model pile cap used in 3-pile pile foundation

Item	Value
Width, B (mm)	80
Length, L (mm)	240
Thickness, t (mm)	30
Pile spacing, s (mm)	80
Normalised pile spacing, s/D	4
Young's modulus, E (MPa)	73,000
Poisson's ratio, ν	0.33

Table 4 Physical and mechanical properties of the model pile cap used in 4-pile pile foundation

Item	Value
Width, B (mm)	100
Length, L (mm)	100
Thickness, t (mm)	30
Pile spacing, s (mm)	50
Normalised pile spacing, s/D	2.5
Density, ρ (g/cm^3)	2.79
Young's modulus, E (MPa)	73,000
Poisson's ratio, ν	0.33

2.2 Model ground

Dry sand that has physical and mechanical properties listed in Table 5 was used for the model ground throughout the experiments. A cylindrical soil box (see Figure 10) was employed for the model ground in the experiment of the single pile and the experiment of the 4-pile pile foundation. For case of the 3-pile pile foundation, a rectangular soil box was used as shown in Figure 11.

Table 5 Properties of the sand used for model ground

Item	Value
Soil particle density, ρ_s (g/cm^3)	2.668
Minimum dry density, ρ_{dmin} (g/cm^3)	1.269
Maximum dry density, ρ_{dmax} (g/cm^3)	1.604
Maximum void ratio, e_{max}	1.103
Minimum void ratio, e_{min}	0.663
Cohesion, c' (kPa)	0
Internal friction angle, ϕ' (degree)	42.8
Poisson's ratio, ν	0.30
Model ground density, ρ (g/cm^3)	1.524
Model ground relative density, D_r (%)	80

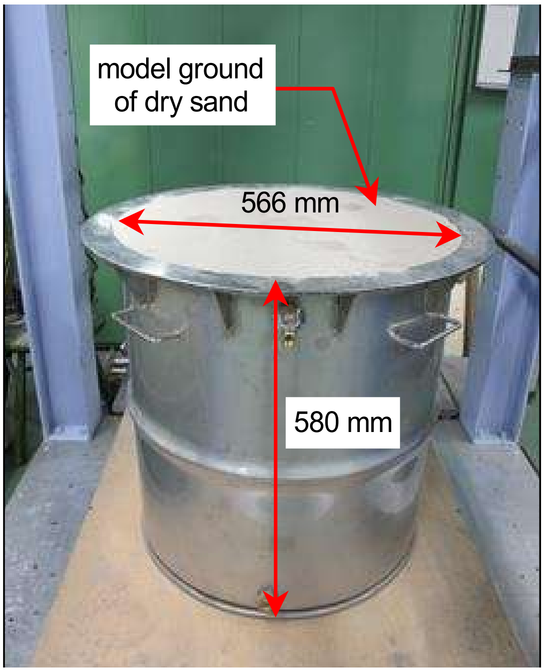

Figure 10 Configurations of the cylindrical model ground container

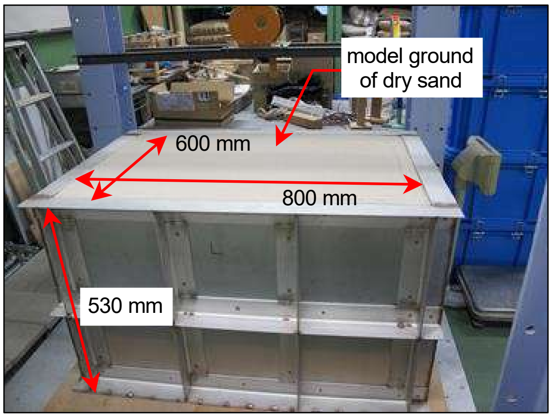

Figure 11 Configurations of the rectangular model ground container

2.3 Model sheet pile walls (SPW)

A PVC (polyvinyl chloride) pipe having 140 mm inner diameter with 135 mm length as shown in Figure 12 was used as model SPW1 in the reinforcement stage of 4-pile pile foundation load tests. Strain gauges were instrumented on the outer surface of SPW1 at symmetric positions (see Figure 12) to measure vertical (axial) and horizontal (hoop) strains during the load tests. Geometrical and mechanical properties of the model SPW1 are listed in Table 6.

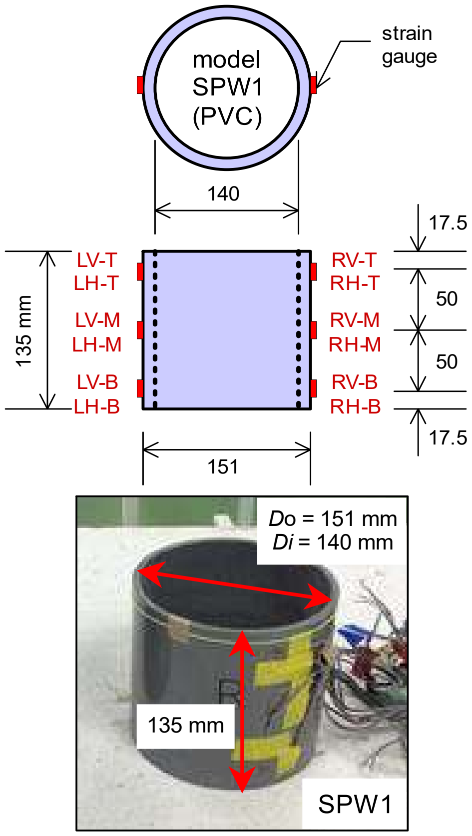

Figure 12 Configurations of the model SPW1

Table 6 Properties of the model SPW1

Item	Value
Outer diameter, D_o (mm)	151
Inner diameter, D_i (mm)	140
Height, H (mm)	135
Wall thickness, t (mm)	5.5
Density, ρ (g/cm^3)	1.415
Young's modulus, E (MPa)	2,100
Poisson's ratio, ν	0.31

Model SPW2 made of PVC pipe having 131 mm inner diameter with 250 mm length as shown in Figure 13 was used in the reinforcement stage of the single pile load tests. The outer surface was instrumented with strain gauges, similarly to the model SPW1. Geometrical and mechanical properties of the model SPW2 are listed in Table 7.

Model SPW3 made of wooden plates having dimensions and configurations as shown in Figure 14 was used in the reinforcement stage of the 3-pile pile foundation load tests. Geometrical and mechanical properties of the model SPW3 are listed in Table 8.

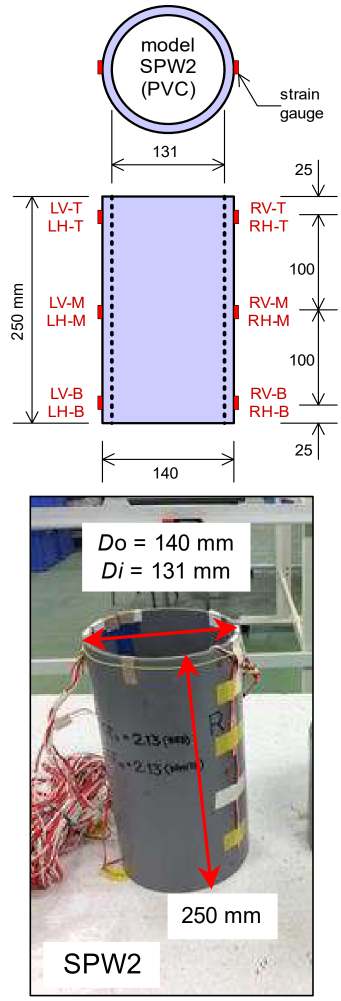

Figure 13 Configurations of the model SPW2

Table 7 Properties of the model SPW2

Item	Value
Outer diameter, D_o (mm)	140
Inner diameter, D_i (mm)	131
Height, H (mm)	250
Wall thickness, t (mm)	4.5
Density, ρ (g/cm^3)	1.415
Young's modulus, E (MPa)	1,900
Poisson's ratio, ν	0.20

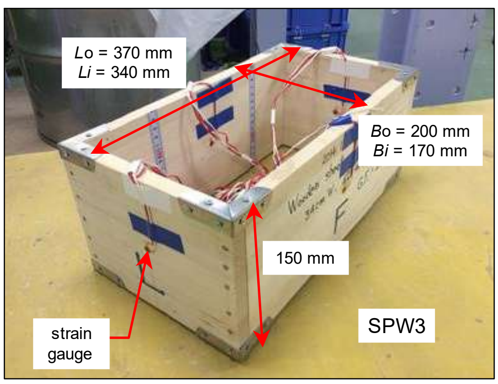

Figure 14 Configurations of the model SPW3

Table 8 Properties of the model SPW3

Item	Value
Outer size, B_o x L_o (mm)	200 x 370
Inner size, B_i x L_i (mm)	170 x 340
Height, H (mm)	150
Wall thickness, t (mm)	15
Young's modulus, E (MPa)	9,500
Poisson's ratio, ν	-

3. EXPERIMENTAL RESULTS

3.1 Vertical load tests on the single pile

In series of vertical load tests (VLTs) on the single pile, VLTs at the initial stage, the embedment reduction stage (simulating riverbed soil excavation) and the reinforcement stage were carried out.

In the preparation of the model ground and the model foundation, the sand was poured into the cylindrical soil container by layers of 50 mm and tamped to have a dry density ρ_d of 1.524 g/cm^3 (D_r = 80%). When the tentative ground surface reached the level of the intended pile tip level, the model foundation was set on the ground surface with support of a jig, and then the sand was again poured into the soil container around the pile and tapped. Finally, the initial condition of the ground having a height of 580 mm and the model preparation was completed. The same procedure was used for the other experiments. The piles for the actual bridges were driven piles. In contrast, the model piles were namely "cast-in-situ" piles. The authors are aware of this discrepancy, but the aim of this study is to investigate the basic mechanism of the SPW reinforcement method. In the reduction stage of pile embedment, the upper ground was removed 4 times with 50 mm thickness in each time as shown in Figure 15 (steps No 2 to No 5).

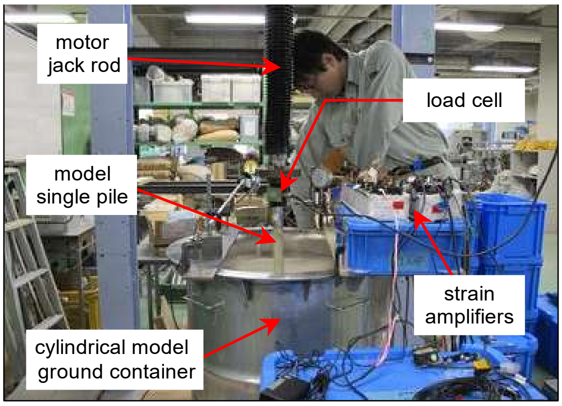

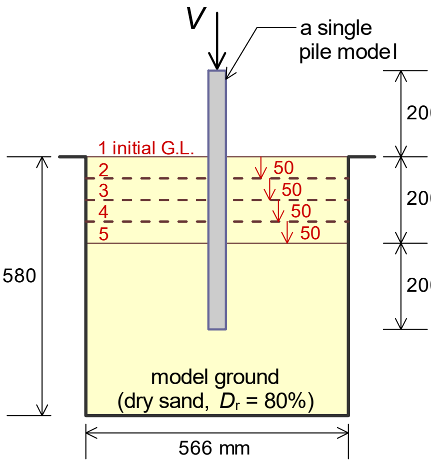

Figure 15 Test conditions and sequences of VLTs on the single pile at the initial stage and in the embedment reduction stage

At step No. 5, the initial embedment length of 400 mm was reduced to 200 mm. After the load test at step No.5, SPW2 (Figure 13) was set on the ground surface. In order to demonstrate confining effects of the SPW, embedment length of the SPW was set to zero. In the reinforcement stage, the inside of SPW2 was refilled with the sand in 3 steps (No. 6 to No. 8) as shown in Figure 16. In the step No. 8, the pile embedment length was recovered to that at the initial condition of 400 mm.

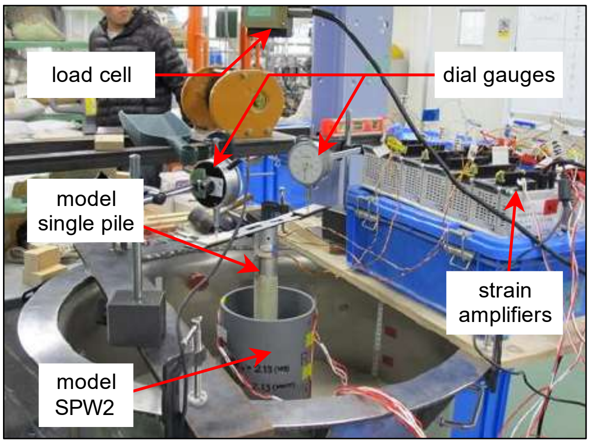

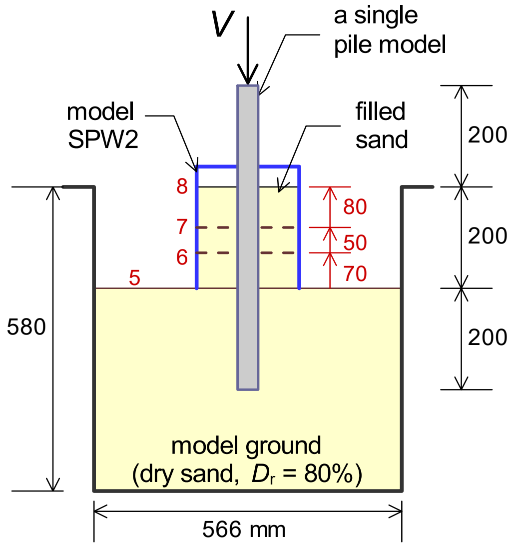

Figure 16 Test conditions and sequences of VLTs on the single pile in the reinforcement stage

Figure 17 shows load-settlement curves at the initial stage No. 1 and in the embedment reduction steps No. 2 to No. 5. It is seen that vertical resistances of the pile decreased with the reductions of pile embedment length from No. 1 to No. 5. Furthermore, though the pile embedment was remaining 50% of the initial condition No. 1 at the final embedment reduction step No. 5, the yield resistance of about 900 N was less than 50% of the yield resistance of 2,100 N at the initial stage No. 1.

Figure 18 shows load-settlement curves at the final embedment reduction step No. 5 and in the reinforcement steps No. 6 to No. 8, comparing with the result at the initial stage No. 1. It is seen that vertical resistance of the pile increased from No. 5 to No. 8 with increasing pile embedment length using the SPW reinforcement. At the final reinforcement step No. 8, the yield resistance of the pile recovered to about 70% of that at the initial stage No. 1 (or to about 140% of that at the final embedment reduction step No. 5).

Figure 19 shows the axial force distributions of the pile in cases of (a) at the initial stage No.1, (b) at the final embedment reduction step No.5 and (c) at the final reinforcement step No. 8. It is seen from the comparison of Figures 19a and 19b that not only shaft friction resistance but also pile tip resistance at the final embedment reduction step No. 5 decreased comparing with those at the initial stage No.1 due to the influence of pile embedment length reduction. At the final reinforcement step No. 8 (Figure 19c), the vertical resistance of the pile was improved due to the recovery of pile embedment length using the SPW reinforcement. However, the pile resistance at the final reinforcement step No. 8 was not fully recovered to that at the initial stage No.1 (Figure 19a).

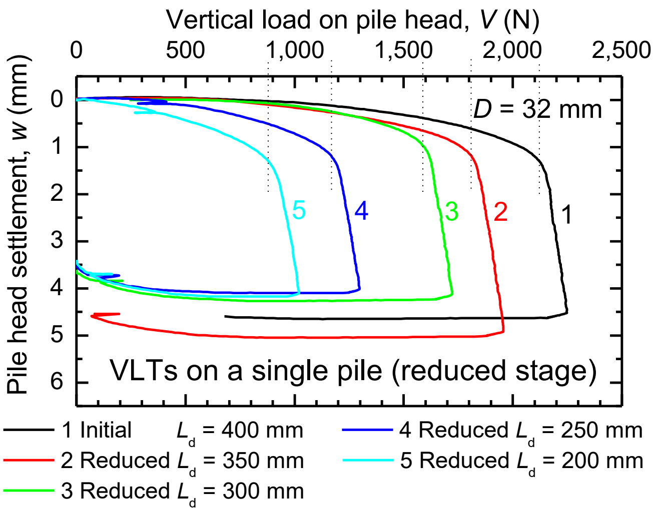

Figure 17 Load-settlement curves of VLTs on the single pile at the initial stage and in the embedment reduction stage

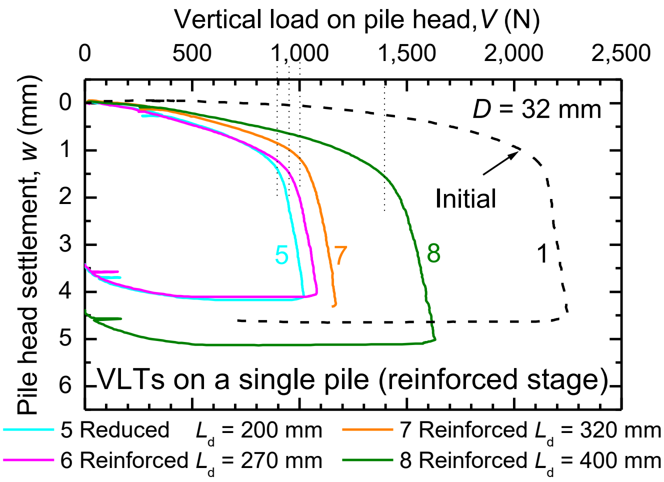

Figure 18 Load-settlement curves of VLTs on the single pile in the reinforcement stage

3.2 Vertical load tests on 3-pile pile foundation

In series of VLTs on the 3-pile pile foundation model, VLTs at the initial stage, in the embedment reduction stage (simulating riverbed soil excavation) and in the reinforcement stage were carried out in similar way to VLTs on the single pile. In the embedment reduction stage, the top ground was removed 4 times (3 times of 50 mm excavation and 1 time of 20 mm excavation) as shown in Figure 20 (steps No. 2 to No. 5). After the load test at step No.5, SPW3 (Figure 14) was set on the ground surface. In the reinforcement stage, the inside of SPW3 was refilled with the sand in 3 steps (No. 6 to No. 8) as shown in Figure 21. In the step No. 8, the pile foundation was recovered to a piled raft foundation where the raft was in contact with the ground surface again.

Figure 22 shows a top view of the arrangement of the model foundation and the model SPW3. The SPW3 was located relatively close to the foundation.

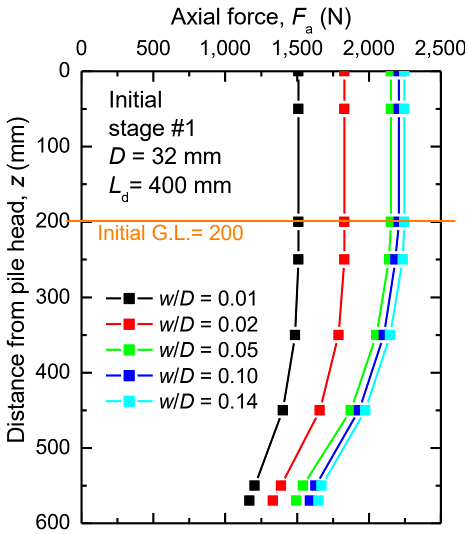

(a) at the initial stage No.1

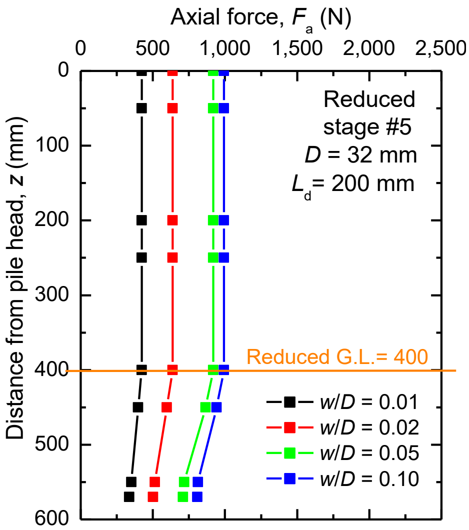

(b) at the final embedment reduction step No.5

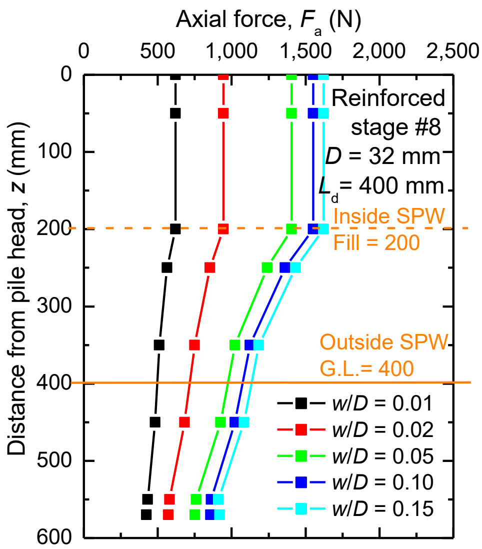

(c) at the final reinforcement step No. 8

Figure 19 Axial force distributions in VLTs on the single pile

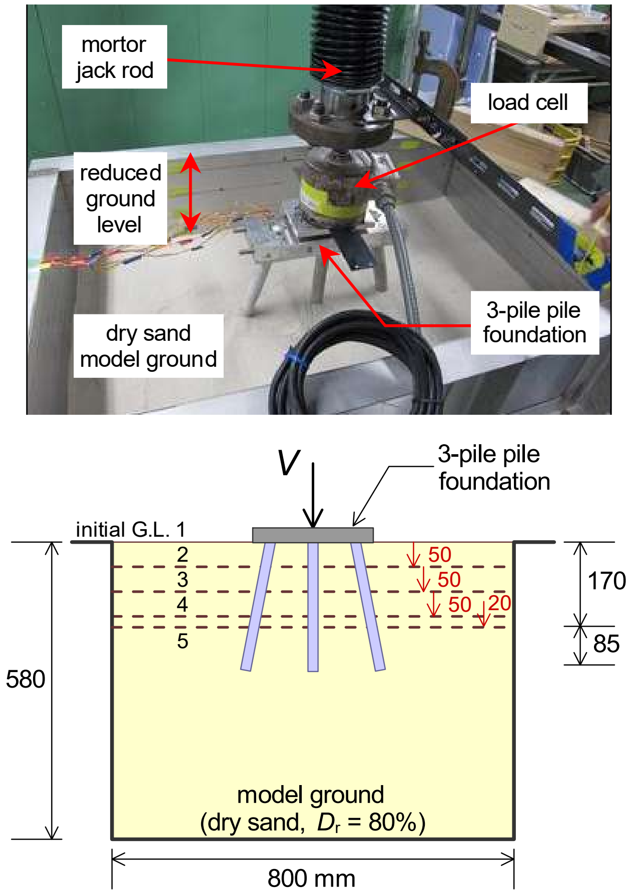

Figure 20 Test conditions of VLTs on 3-pile pile foundation at the initial stage and the embedment reduction stage

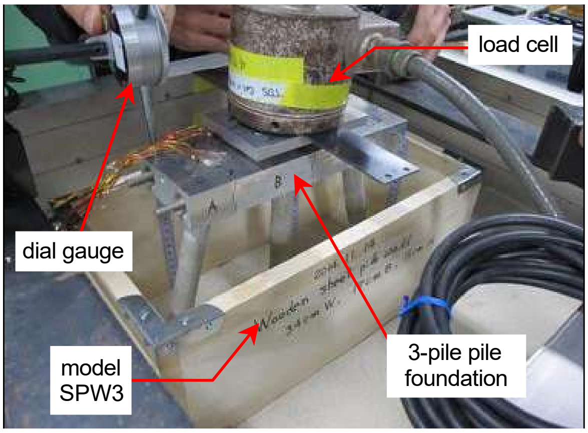

Foundation, VLTs on the 4-

Figure 21 Test conditions of VLTs on 3-pile pile foundation in the reinforcement stage

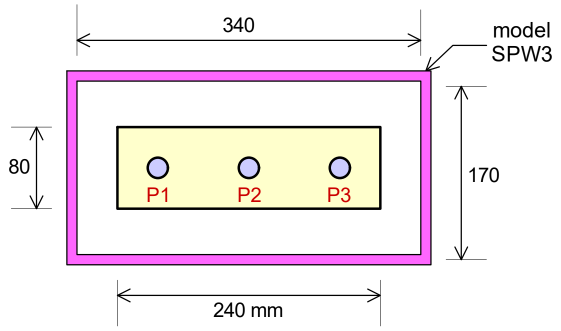

Figures 22 Top view dimensions of SPW reinforcement in VLTs on 3-pile pile foundation

Figure 23 shows load-settlement curves at the initial stage No. 1 and in the embedment reduction steps No. 2 to No. 5. It is seen that the vertical resistance as well as stiffness of the 3-pile pile foundation decreased from No. 1 to No. 5 with the reduction of pile embedment length. It should be noted that the reduction of the resistance from the initial condition No. 1 to the embedment reduction step No. 2 was notably larger compared with those in the sequent reduction steps. The large reduction of the resistance at step No. 2 was caused by mainly the loss of raft resistance. Namely, the foundation type changed from a piled raft at the initial stage No. 1 into a pile group in steps No. 2 to No. 5. The reduction of foundation resistance from steps No. 2 to No. 5 was due to the reduction of pile resistance.

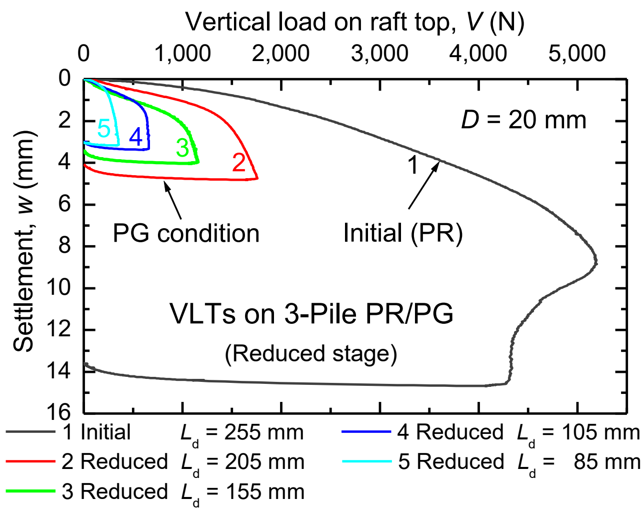

Figure 23 Load-settlement curves of VLTs on 3-pile pile foundation at the initial stage and the embedment reduction stage

Figure 24 shows load-settlement curves in the reinforcement steps No. 6 to No. 8, comparing with the results at the final embedment reduction step No. 5 and the initial stage No. 1. It is seen that the vertical resistance and stiffness of the 3-pile pile foundation increased from step No. 5 to step No. 8 with the increase of pile embedment length using the SPW reinforcement. Particularly, the recovery of the resistance from step No. 7 to step No. 8 was noticeable due to the recovery of the raft resistance at step No. 8. The load-settlement curve at step No. 8 recovered nearly to that at the initial stage.

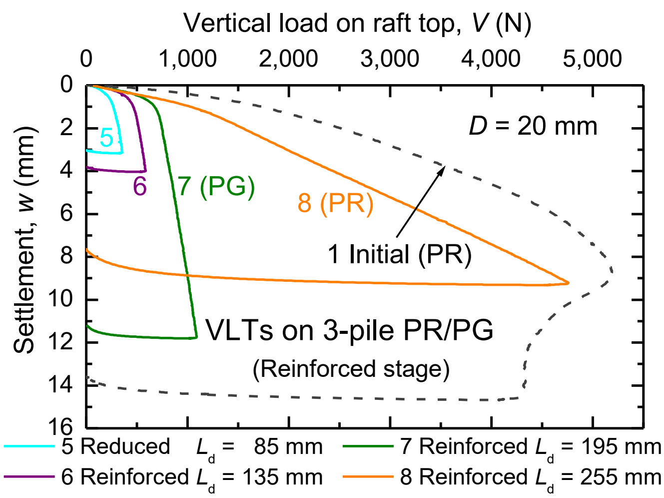

Figure 24 Load-settlement curves of VLTs on 3-pile pile foundation in the reinforcement stage

3.3 Vertical load tests on 4-pile pile foundation

Similar to the VLTs on the single pile and the 3-pile pile foundation, VLTs on the 4-pile pile foundation were carried out at the initial condition and in each stage of the pile embedment length reduction and the SPW reinforcement, as shown in Figure 25 (reduction stage) and Figure 26 (reinforcement stage). In the reinforcement stage, SPW1 (Figure 12) was located very close to the model foundation, as shown in Figure 27. It is desirable to minimize the size of the SPW so that the SPW structure does not interfere river stream as much as possible when the SPW reinforcement is applied to an actual bridge foundation.

Figure 28 shows load-settlement curves at the initial stage No.1 and in the embedment reduction steps No. 2 to No. 4. Note here that settlement was zeroed at the start of loading in each step for comparison. It is seen that vertical resistances and initial stiffness of the pile foundation decreased with the reduction of pile embedment length from No. 2 to No. 4. It is also seen that the load-settlement curves in the reduction steps No. 2 and No. 3 exhibit a plunging behaviour and the response in step No. 4 exhibits a softening behaviour, while the response at the initial stage No. 1 shows a progressive failure behaviour.

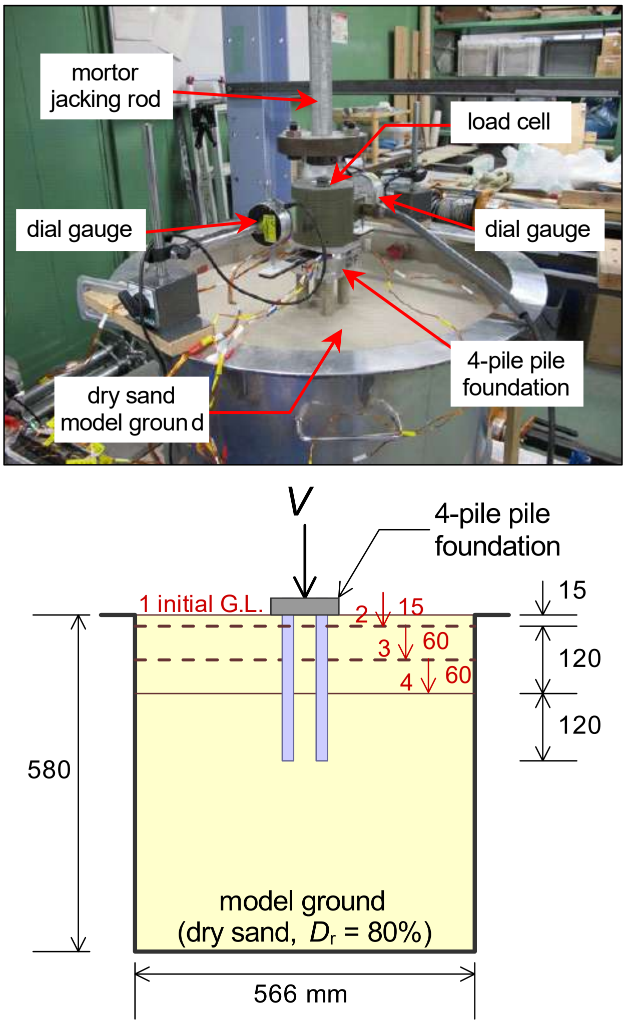

Figure 25 Test conditions of VLTs on 4-pile pile foundation at the initial stage and in the embedment reduction stage

Figure 29 shows load-settlement curves in the reinforcement steps No.5 to No.7, comparing with the results at the final embedment reduction step No.4 and the initial stage No. 1. It is seen that the vertical resistance and stiffness of the 4-pile pile foundation increased from step No. 4 to step No. 7 with increasing pile embedment length using the SPW reinforcement. In particular, the vertical resistance at the final reinforcement step No. 7 was much greater than that of the initial stage No. 1.

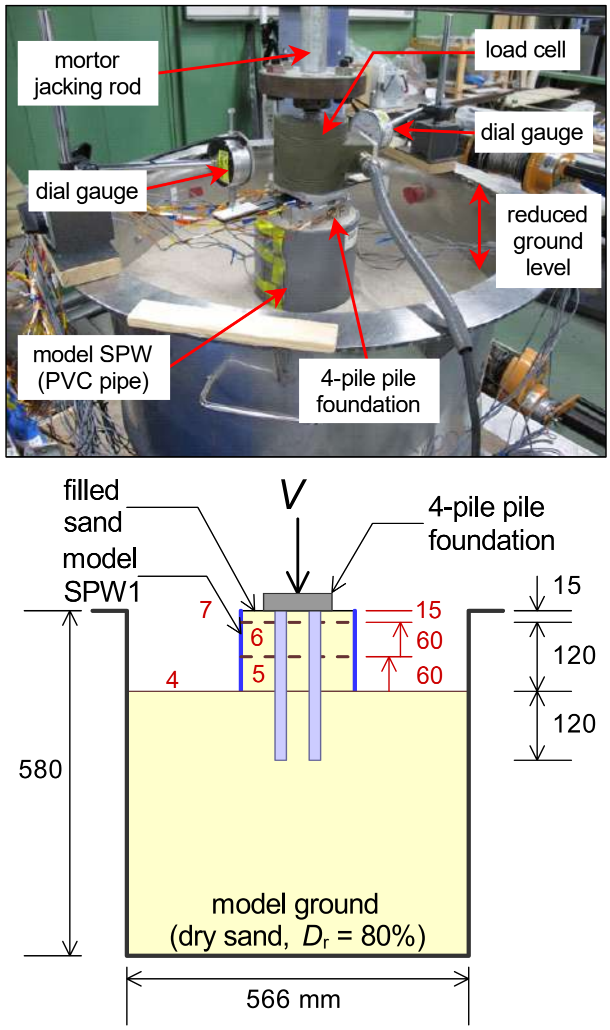

Figure 26 Test conditions of VLTs on 4-pile pile foundation in the reinforcement stage

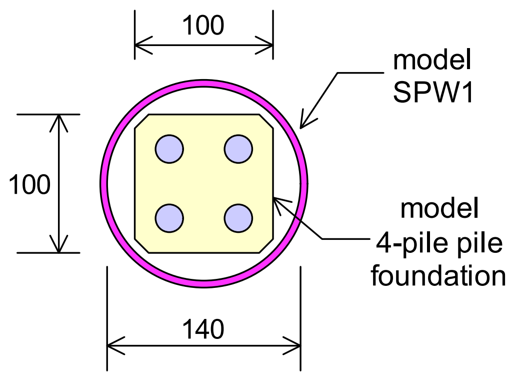

Figure 27 Top view dimensions of SPW reinforcement in VLTs on 4-pile pile foundation

Figures 30 and 31 show the loads carried by the 4 piles and the raft at the initial stage (step No. 1) and at step No. 7 (the final reinforcement), respectively. It is seen from the comparison of both figures that the vertical resistances of both the raft and the 4 piles increased by approximately double, comparing step No. 7 with step No. 1, showing a considerable effect of the SPW reinforcement.

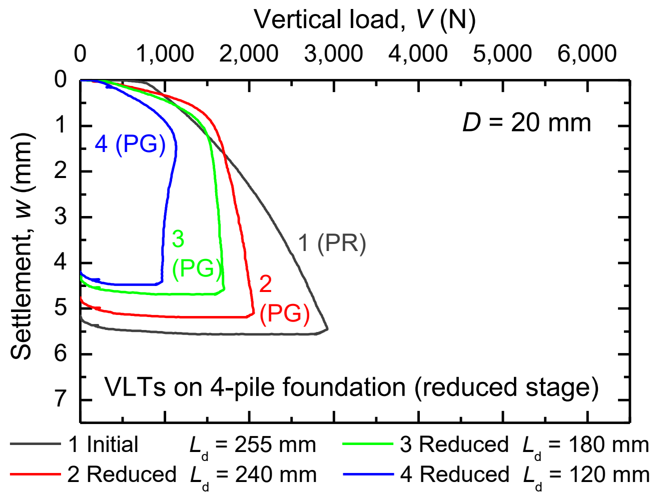

Figure 28 Load-settlement curves of VLTs on 4-pile pile foundation at the initial stage and in the stage of pile embedment reduction

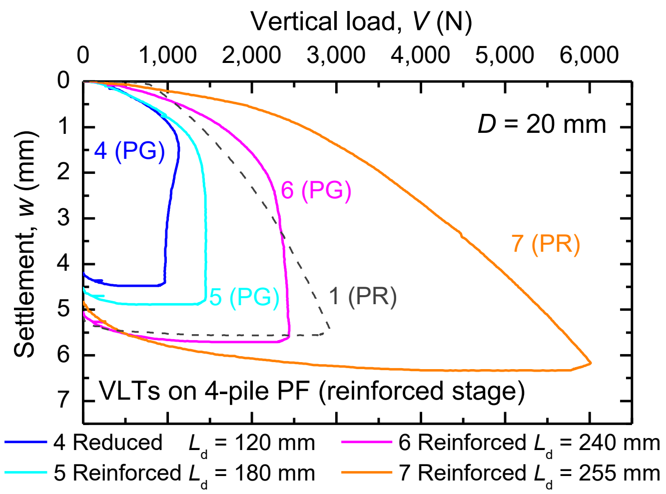

Figure 29 Load-settlement curves of VLTs on 4-pile pile foundation in the reinforcement stage

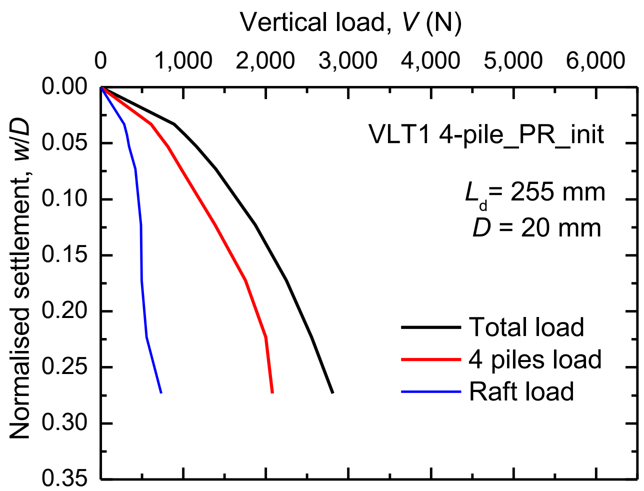

Figure 30 Loads carried by the piles and the raft at the initial stage No. 1

Figures 32 and 33 show changes of distributions of axial (vertical) strains and hoop (horizontal) strains of the SPW with increasing normalised settlement of the foundation, w/D, where w is the settlement and D is the pile diameter, respectively, during load test at the final reinforcement step No. 7. Note that compression strain is taken as positive and tension strain is taken as negative. Since the experiment is essentially axi-symmetric problem, averages of the measured strains at the opposite sides of the SPW were taken in Figures 32 and 33.

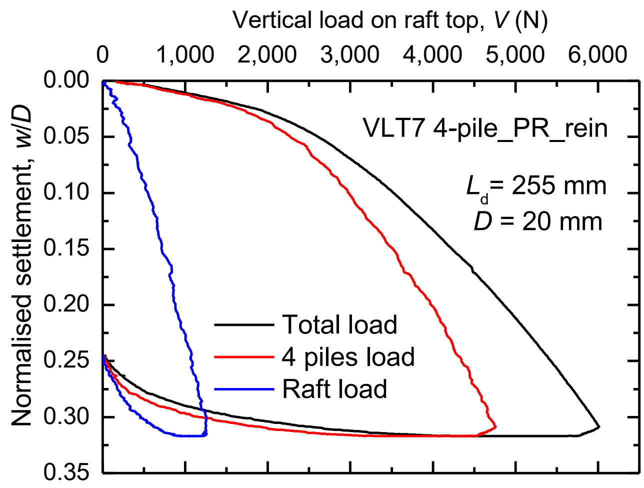

Figure 31 Loads carried by the piles and the raft at the final reinforcement No. 7

It is seen that the maximum values of both axial strain and hoop strain were generated around the SPW base. It is also seen that absolute magnitudes of the hoop strains are larger than those of the axial strains at each w/D. This means that the soil inside the SPW is subjected to large horizontal stresses by the existence of SPW. Hence, it is reasonable that the foundation, especially the raft component, at step No. 7 has the larger resistance than that of the initial stage.

Although the direct estimation of the horizontal stresses of the soil inside the SPW from the measured axial and horizontal strains of the SPW is difficult, the results of Figures 32 and 33 indicate that larger vertical and horizontal stresses are generated in the soil inside the SPW at step No. 7.

If SPW having zig-zag section of steel sheet piles with interlocks is used in practice, similar effects of the SPW could be expected, although different stiffness of the PVC wall and the steel sheet pile wall should be taken into account.

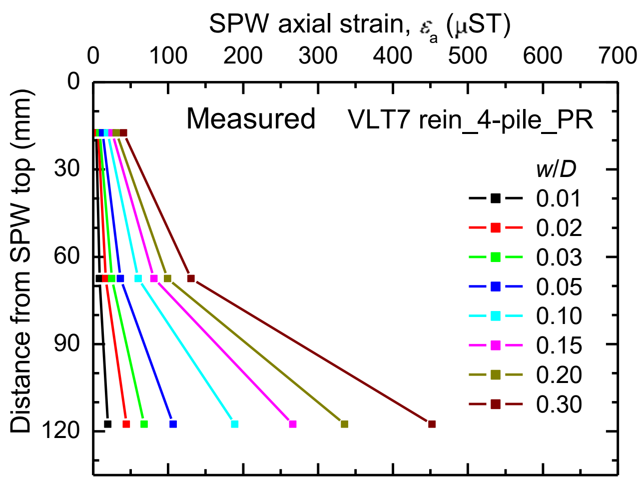

Figure 32 SPW axial strain distributions in the final reinforcement stage of VLTs on 4-pile pile foundation

Figure 34 shows a conceptual expression of stress transfer from the raft base to the soil inside the SPW. A part of the vertical load on the foundation is supported by the raft. The vertical load supported by the raft base is transferred to the soil inside the SPW. The horizontal stresses as well as vertical stress in the soil are increased by the increase in the raft base stresses due to the existence of the SPW. Hence, it seems to be reasonable that the raft resistance after the construction of the SPW becomes larger than that at the initial condition. It is inferred from the experimental results that efficiency of the SPW reinforcement is governed by size (distance) relative to the existing foundation, and stiffness of the SPW as well as stiffness of the soil inside the SPW.

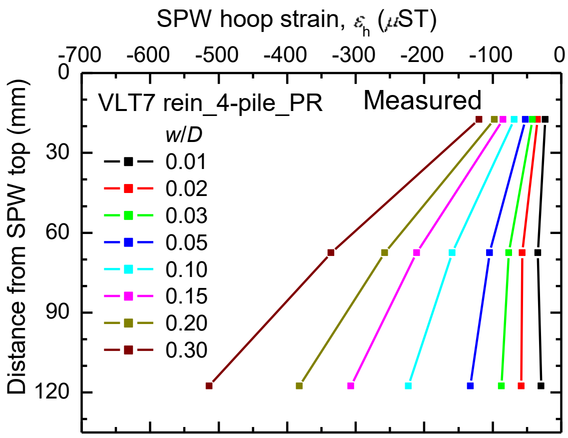

Figure 33 SPW hoop strain distributions in the final reinforcement stage of VLTs on 4-pile pile foundation

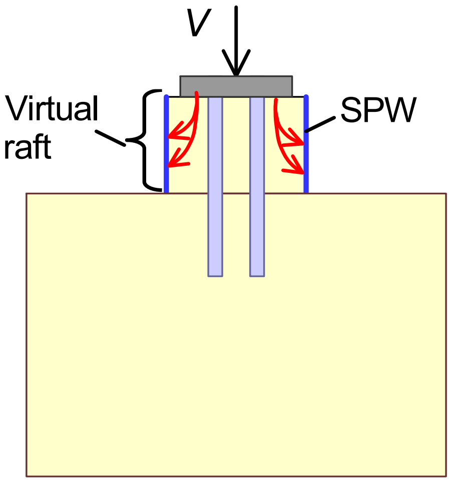

Figure 34 Conceptual expression of stress transfer from the raft to the soil inside the SPW

4. NUMERICAL STUDY

FEM simulation of the vertical load tests on the 4-pile pile foundation was carried out to get more insight into the reinforcement mechanism and to explore a possible method to predict the experimental results for a design purpose.

4.1 CD triaxial tests of the sand and simulation

A series of Consolidated Drained Shear tests (CD tests) of the sand with different confining pressures were carried out in order to select an appropriate soil model and to estimate the soil parameters (Vu et al., 2017), because it was expected that stiffness and dilatancy behaviour of the sand are dependent on stress level. The height and diameter of the soil specimens were 100 mm and 50 mm, respectively. The drainage from the specimen was permitted from only the top end. The isotropic confining pressures, p_0, used were 7, 17, 27 and 50 kPa. Note that the effective vertical stress at the bottom of the model ground was about 7.5 kPa.

Figure 35 shows the results of the CD tests. It is seen from Figure 35a that the sand exhibits post-peak strain softening behaviours in each p_0 and that the stiffness ($\Delta q/\Delta\varepsilon_a$) prior to the peak q increases with increasing p_0. It is seen from Figure 35b that the sand exhibits a positive dilatancy, and dilatancy angle is not constant but decreases with increasing ε_a, and that degree of positive dilatancy decreases with increasing p_0. In order to simulate such CD test results, the Hypoplastic model, an incrementally nonlinear constitutive model, was employed.

The early version of Hypoplastic model was introduced by Kolymbas (1985), which describes the stress-strain behaviour of granular materials in a rate form. After that, modifications and implementations of the model were proposed by Gudehus (1996), Wolffersdorff (1996), and Masin (2005). The basic Hypoplastic model for granular materials includes eight parameters such as critical friction angle φ_c, granular hardness h_s, exponents n, α and β, and minimum, maximum and critical void ratios at zero pressure e_{d0}, e_{i0} and e_{c0}. A shortcoming of the basic Hypoplastic model is over prediction of accumulated deformation due to cyclic loading. Niemunis and Herle (1997) introduced an extended Hypoplastic model to improve the performance of the basic Hypoplastic model in cyclic loading. Five additional parameters are required in the extended Hypoplastic model such as stiffness multiplier for initial and reverse loading m_R, stiffness multiplier for neutral loading m_T, small strain stiffness limit R_{max}, parameters adjusting stiffness reduction β_r and χ.

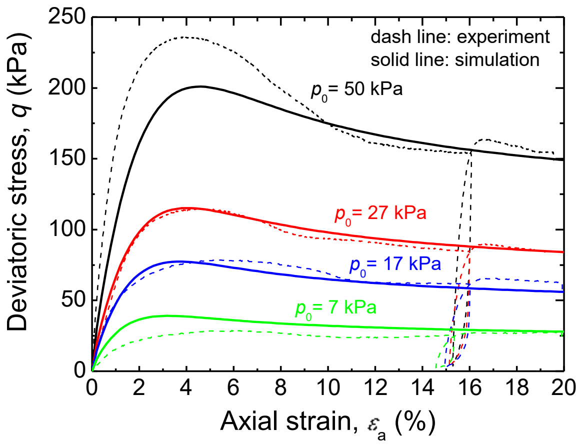

(a) Deviatoric stress, q versus axial strain, ε_a

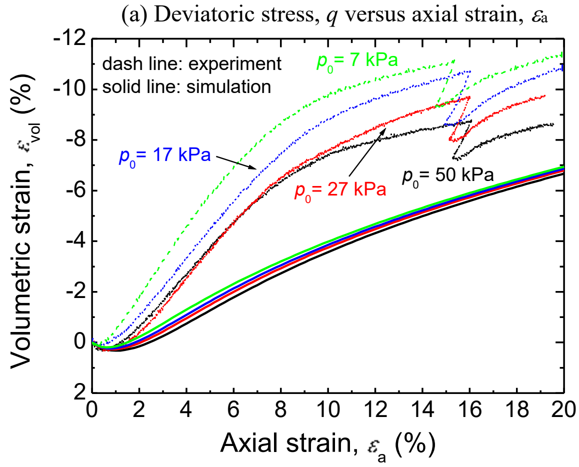

(b) Volumetric strain, ε_{vol} versus axial strain, ε_a

Figure 35 Results of the triaxial CD tests and simulations using the Hypoplastic soil model

The results of the simulations are indicated in Figure 35. The soil parameters used in the simulations are listed in Table 9. These soil parameters were determined so that the calculated results match with the results of the CD tests with smaller values of p_0 (p_0 = 7, 17 and 27 kPa), because the effective vertical stress at the bottom of the model ground was about 7.5 kPa as mentioned earlier. Although the calculated result for the CD test with p_0 = 50 kPa underestimates the peak value of q, the calculated result well simulates the overall trend of the measured results. It is seen from Figure 35b that the calculated results underestimate the measured positive dilatancy, but well simulate the tendency of the measured dilatancy behaviours.

4.2 FEM simulation of VLTs on the 4-pile pile foundation

A half of the model ground and the foundation was modelled in FEM analysis, because of the symmetric condition of the experiment. The authors are aware that it is possible to model only one-fourth of the ground and the foundation in case of the vertical load tests. Modelling the half of the ground and the foundation was adopted for analysis of horizontal loading in future.

The FEM meshes of the foundation and the ground in each step are shown in Figure 36. Displacements in y-direction on the symmetric plane, displacements in z-direction on the bottom surface, and displacements in x- and y-directions on the cylindrical outer surface of the ground were fixed, according to the experimental conditions.

The raft and the piles were considered as linear elastic materials. In order to model the piles, a hybrid model in which beam elements surrounded by solid elements was employed, following Kimura and Zhang (2000). Figure 37 shows the mechanism of the hybrid model. In the hybrid model of this research, beam element carried large proportion (90%) of the bending stiffness, EI, and axial stiffness, EA, of the pile. The properties of the raft, the beam, the solid pile and the weight plates are summarised in Table 10.

Interface elements of Mohr-Coulomb type were assigned at the raft base and the pile shafts. Interface cohesion was set 0, and the interface friction angle of 40.2 degrees was used following Unsever et al. (2015).

The following FEM analysis procedure was adopted:

(1): K_0 consolidation of the ground alone.

(2): Setting the foundation in the model ground and gravity (self-weight) calculation.

(3): Calculation of loading and unloading processes in Step 1 (SLT at the initial condition). Note that a prescribed vertical displacement was applied on the raft in the loading process, and then the prescribed displacement was released in the unloading process.

(4): Calculation of soil excavation, then calculation of loading and unloading processes of the foundation in steps No. 2 to No. 4.

(5): Setting the SPW, and calculation of refilling the soil inside the SPW, and then calculation of loading and unloading processes in steps No. 5 to No. 7.

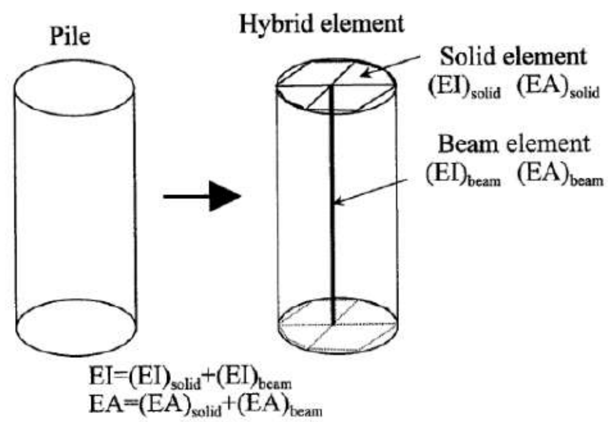

Figure 37 Mechanism of the hybrid model (after Kimura and Zhang, 2000)

The calculated and measured load-displacement curves are compared in Figure 38. The calculated results are comparable to the measured results except for step No. 7. In the refilling of the sand beneath the raft prior to step No. 7 in the experiment, the sand was pushed into the space between the ground surface and the raft base very hardly by tapping using a slender bar. This procedure may have caused the sand inside the SPW over-tamped. But, it is difficult at present to derive an exact reason for the discrepancy between the measured and calculated results for step No. 7 only.

Figure 39 shows the comparison of calculated and measured load sharing in the vertical load tests at step No. 1 and step No. 7. Note here that the vertical displacement was zeroed at the start of Step 7 for a purpose of comparison between Figures 39a and 39b. Similar to the measured results, it is seen from the calculation results that both the raft resistance and the pile resistance increase in step No. 7, comparing with step No. 1. However, the calculated value of the pile resistance is smaller than the measured value at a given settlement. This result corresponds to the smaller stiffness of the calculated load-settlement curve that was shown in Figure 38.

Figure 40 compares the calculated and measured vertical strains of the SPW at step No. 7. Similarly, Figure 41 compares the calculated and measured hoop strains of the SPW at step No. 7. The calculation results well simulate the measured results in which the amplitudes of vertical strains (in compression) and the hoop strains (in tension) increases with increasing the foundation settlement and these amplitudes increase from the top to the bottom of SPW. Relatively large amplitudes of the hoop strains indicate the increase of the confining pressure in the refilled soil inside the SPW.

Table 9 Parameters of the Hypoplastic model identified from the simulations of triaxial CD tests

φ_c (deg.)	h_s (N/mm^2)	n	e_{d0}	e_{c0}	e_{i0}	α	β	m_R	m_T	R_{max}	β_r	χ	p_t (N/mm^2)	e
31	2000	0.28	0.663	1.1	1.2	0.10	1.2	5	2	5×10^{-5}	0.5	1	3×10^{-3}	0.739

Table 10 Properties of the elastic elements

	Beam	Solid pile	Raft
Unit weight, γ (N/mm^3)	2.381×10^{-5}	5.501×10^{-7}	2.650×10^{-5}
Young's modulus, E (N/mm^2)	63.24×10^3	14.61×10^2	68.67×10^3
Poisson's ratio, ν	0.31	-	0.33

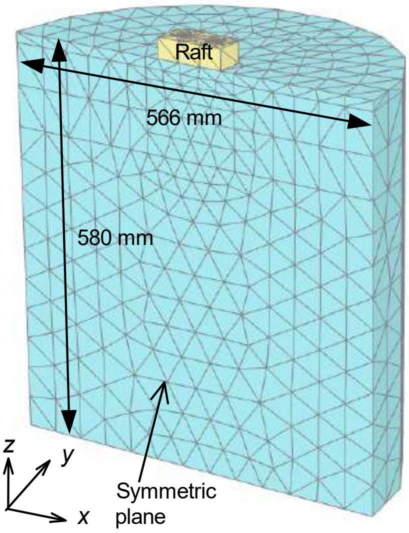

(a) Step 1 at the initial stage

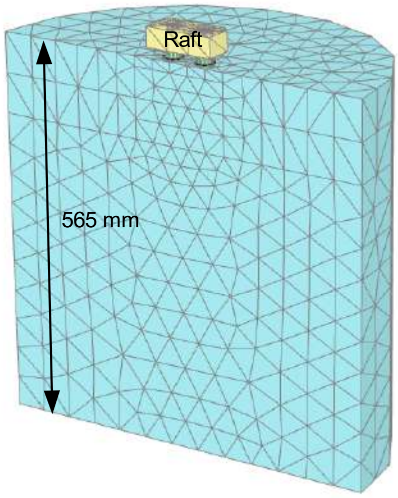

(b) Step 2 in reduction stage

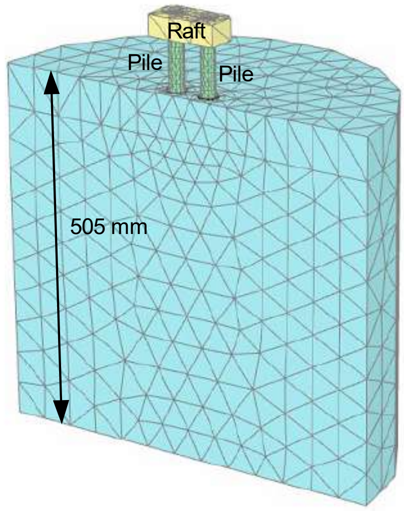

(c) Step 3 in reduction stage

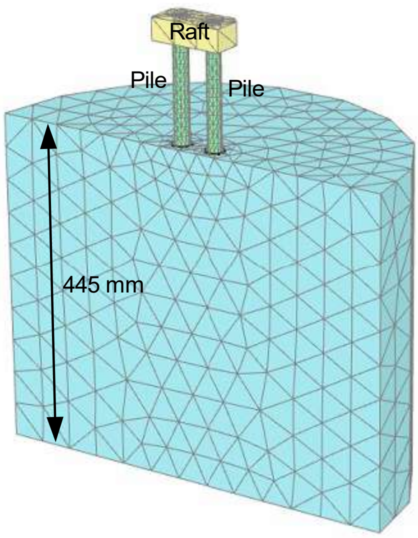

(d) Step 4 in reduction stage

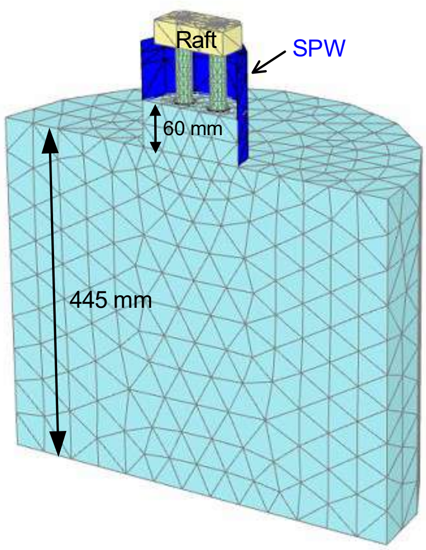

(e) Step 5 in reinforcement stage

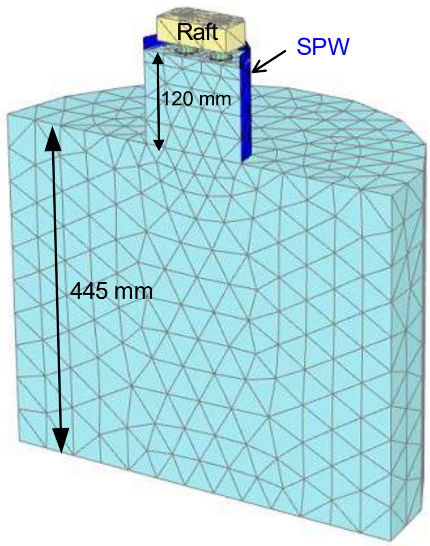

(f) Step 6 in reinforcement stage

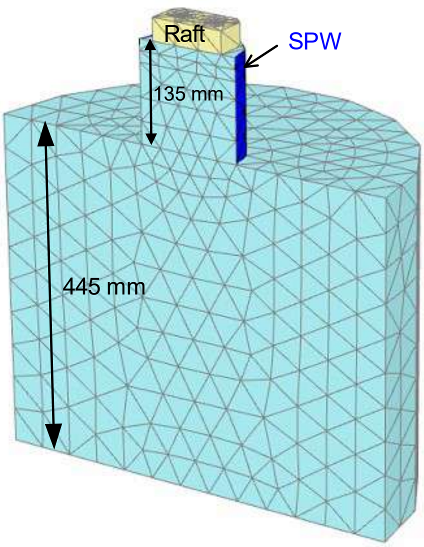

(g) Step 7 in reinforcement stage

Figure 36 FEM meshes for the ground and the 4-pile pile foundation

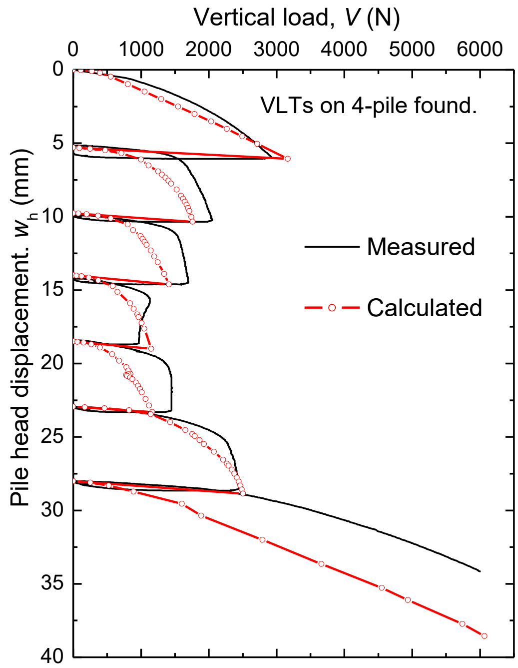

Figure 38 Comparison of calculated and measured load-displacement relation of the 4-pile pile foundation

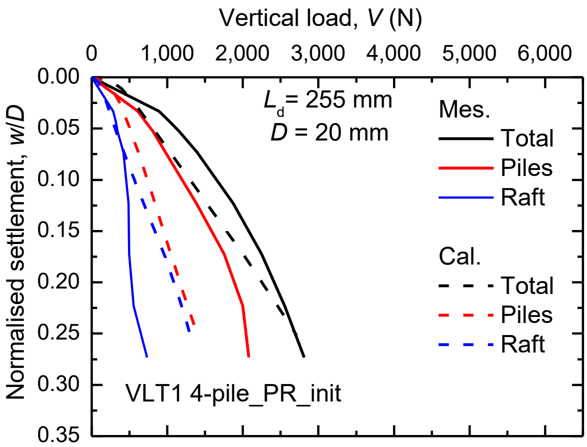

(a) Step 1 (Vertical loading at the initial stage)

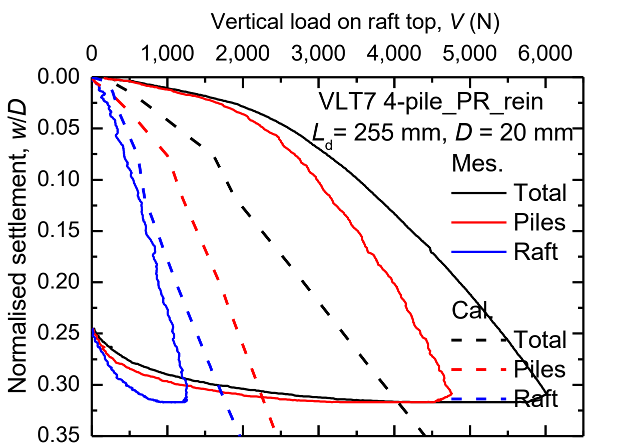

(b) Step 7 (Vertical loading at the final reinforcement stage)

Figure 39 Comparison of measured and calculated load sharing in the vertical load tests at Step 1 and Step 7

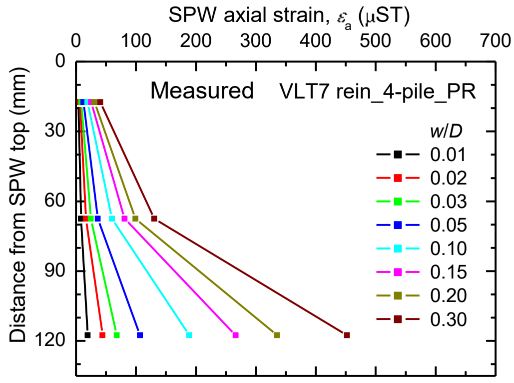

(a) measured (Figure 32 repeated)

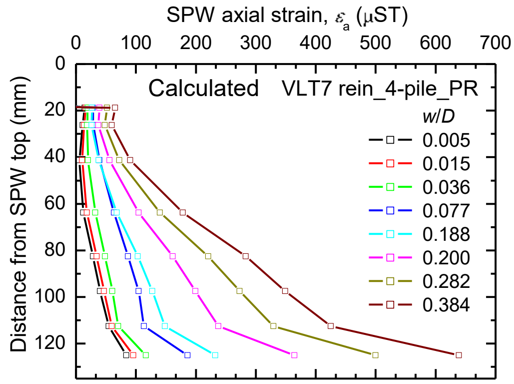

(b) calculated

Figure 40 Comparison of measured and calculated hoop strains of the SPW in Step 7

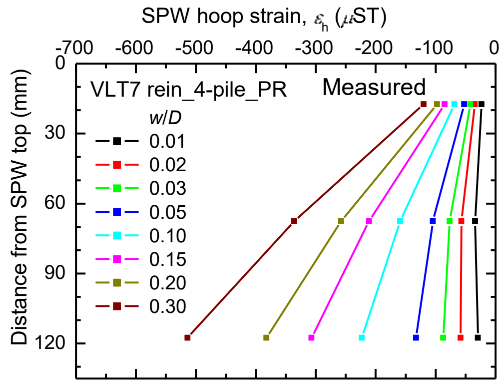

(a) measured (Figure 33 repeated)

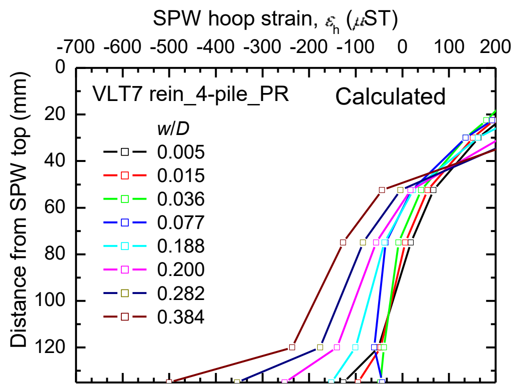

(b) calculated

Figure 41 Comparison of measured and calculated hoop strains of the SPW in Step 7

5. CONCLUSIONS

In order to search for a practical method for reinforcing the existing bridge pile foundations in Thailand that have been subjected to reduction of pile embedment length due to riverbed excavation, series of vertical load tests on model pile foundations were carried out in dry sand ground. An initial condition of the model foundation, the reduction stage of the pile embedment length and the reinforcement stage of the pile foundation were simulated in the experiments. The pile foundation subjected to pile embedment length is reinforced using the sheet pile wall surrounding the foundation with filling soils inside the sheet pile wall. The reinforcement method is named "SPW reinforce method".

The validity of the SPW method was examined through vertical loading on a single pile model, 3-pile pile foundation model and 4-pile pile foundation model. It was demonstrated from the experiments that the SPW reinforcement method is very efficient and promising. FEM simulation was also carried out for the load tests on the 4-pile pile foundation model, to validate the SPW reinforcement method and to get more insight into the mechanism of the SPW reinforcement method.

Main findings from the experiments and the numerical simulation are:

(1) A significant reduction of the pile foundation resistance is caused by the loss of the vertical resistance of the raft due to a small amount of the soil excavation beneath the raft.
(2) After that, the foundation resistance decreases with increasing the depth of the soil excavation, in other words, with decreasing pile embedment length.
(3) The resistance of the 3-pile pile foundation reinforced by the SPW method almost recovered to the resistance at the initial condition. The 4-pile pile foundation reinforced by the SPW method exhibits higher resistance than the pile foundation at the initial condition.
(4) An important mechanism of the SPW reinforcement method is that the filled soil inside the SPW are effectively confined by the stress transfer from the raft base and the SPW.

The foundations of the Mae Nam Ping River crossing bridges lose the raft resistance at present due to riverbed excavation. Hence, recovering of the raft resistance using the proposed SPW method would be a promising counter measure to prevent damages.

It is inferred from the experimental results that radius (size) of the SPW relative to the raft, tension stiffness of the SPW as well as the stiffness of the filled soil are key factors for the efficiency of the SPW reinforce method.

The following items are future subjects in this research:

(1) Numerical parametric study to investigate the influence of the radius (size) of the SPW relative to the foundation size.
(2) In order to investigate the influences of flood load and scouring, and to validate the proposed reinforcing method, a full scale field test would be beneficial.

6. ACKNOWLEDGEMENTS

The authors would like to express profound gratitude to International Press-in Association (IPA) for their financial support provided to this research.

7. REFERENCES

Fukada, H., Kato, K., Aoyagi, M., Inagawa, H, and Shioi, Y. (2005) "Application of Reinforcing Methods for Existing Pile Foundation on Soft Ground (In-cap Method)", Public Works Research Institute: The 23th US - Japan Bridge Engineering Workshop. Retrieved July 1, 2014.

Gudehus, G. (1996) "A comprehensive constitutive equation for granular materials", Soils and Foundations, 36(1), pp1-12.

Kimura, M., and Zhang, F. (2000) "Seismic evaluation of pile foundations with three different methods based on three-dimensional elasto-plastic finite element analysis", Soils and Foundations, 40(5), pp113-132.

Niemunis A, and Herle I. (1997) "Hypoplastic model for cohesionless soils with elastic strain range". Mechanics of cohesive-frictional materials, 2, pp279-299.

Unsever, Y. S., Matsumoto, T., and Ozkan, M. Y. (2015). "Numerical analyses of load tests on model foundations in dry sand", Computers and Geotechnics, 63, pp40-51.

Vu, A.T., Matsumoto, T., Shimono, S., and Nguyen, T. L. (2017) "Model load tests on battered pile foundations and finite-element analysis", Int. Journal of Physical Modelling in Geotechnics, published online on 2016 Nov 30th, 22 pages, http://dx.doi.org/10.1680/jphmg.16.00010.

Kolymbas, D. (1985) "A generalized hypoelastic constitutive law", Proc. of Int. Conf. on Soil Mechanics and Foundation Engineering, San Francisco, 5, pp2626.

Masin, D. (2005) "A hypoplastic constitutive model for clays", Int. Journal for Numerical and Analytical Methods in Geomechanics, 24(4), pp311-336.

Wolffersdorff, P. A. (1996) "A hypoplastic relation for granular materials with a predefined limit state surface", Mechanics of cohesive-frictional materials, 1, pp251-271.